J Biomol NMR (2014) 58:27–35
DOI 10.1007/s10858-013-9800-4

ARTICLE

Paramagnetic doping of a 7TM membrane protein in lipid bilayers by Gd^{3+}-complexes for solid-state NMR spectroscopy

Sandra J. Ullrich · Soraya Hölper · Clemens Glaubitz

Received: 22 September 2013 / Accepted: 26 November 2013 / Published online: 4 December 2013

Abstract A considerable limitation of NMR spectroscopy is its inherent low sensitivity. Approximately 90 % of the measuring time is used by the spin system to return to its Boltzmann equilibrium after excitation, which is determined by ^{1}H-T_1 in cross-polarized solid-state NMR experiments. It has been shown that sample doping by paramagnetic relaxation agents such as Cu^{2+}-EDTA accelerates this process considerably resulting in enhanced sensitivity. Here, we extend this concept to Gd^{3+}-complexes. Their effect on ^{1}H-T_1 has been assessed on the membrane protein proteorhodopsin, a 7TM light-driven proton pump. A comparison between Gd^{3+}-DOTA, Gd^{3+}-TTAHA, covalently attached Cu^{2+}-EDTA-tags and Cu^{2+}-EDTA reveals a 3.2-, 2.6-, 2.4- and 2-fold improved signal-to-noise ratio per unit time due to longitudinal paramagnetic relaxation enhancement. Furthermore, Gd^{3+}-DOTA shows a remarkably high relaxivity, which is 77-times higher than that of Cu^{2+}-EDTA. Therefore, an order of magnitude lower dopant concentration can be used. In addition, no line-broadening effects or peak shifts have been observed on proteorhodopsin in the presence of Gd^{3+}-DOTA. These favourable properties make it very useful for solid-state NMR experiments on membrane proteins.

Keywords Solid-state NMR · MAS · PRE · Gd-DOTA

Electronic supplementary material The online version of this article (doi:10.1007/s10858-013-9800-4) contains supplementary material, which is available to authorized users.

S. J. Ullrich · S. Hölper · C. Glaubitz (✉)
Institute for Biophysical Chemistry, Centre for Biomolecular Magnetic Resonance, Goethe-University Frankfurt, Max von Laue Str. 9, 60438 Frankfurt am Main, Germany
e-mail: glaubitz@em.uni-frankfurt.de

Introduction

Solid-state NMR is a powerful method to gain insight into structure and functional mechanisms of membrane proteins or other insoluble macromolecular complexes (Renault et al. 2010). Unfortunately, NMR in general and solid-state NMR in particular suffers from low inherent sensitivity. This is especially true in case of membrane protein applications due to their limited spin concentration, which results in long data collection times needed to accumulate a sufficient signal-to-noise ratio (SNR). Almost 90 % of the experimental time is required to restore the ^{1}H Boltzmann equilibrium after each cross-polarization step. The necessary recycle delay equals 4–5-times the ^{1}H longitudinal relaxation time (^{1}H-T_1), which is usually also needed to limit the probehead duty cycle and to avoid unnecessary sample heating. One possible route for enhancing the SNR per unit time is to reduce ^{1}H-T_1 by doping the sample with paramagnetic relaxation agents (Ganapathy et al. 1981). So far, Cu^{2+}-EDTA has been used successfully for a multitude of samples facilitating rapid data acquisition with increased sensitivity. Examples include microcrystalline proteins (Linser et al. 2007; Wickramasinghe et al. 2009), membrane proteins (Tang et al. 2011; Yamamoto et al. 2010) and complex biomaterials (Mroue et al. 2012). In case of membrane application, copper-chelated lipids have been used and the enhanced SNR per unit time even enabled detecting unlabelled peptides within bicelles (Yamamoto et al. 2010, 2011). This work resulted in a general approach termed paramagnetic relaxation-assisted condensed data collection (PACC) (Ganapathy et al. 1981; Parthasarathy et al. 2013; Wickramasinghe et al. 2007, 2008, 2009), which combines paramagnetic doping with Cu^{2+}-EDTA, rapid MAS ($\geq$40 kHz), low power decoupling and short recycle delays. It was also demonstrated, that the intrinsic

Table 1 Summary of dopant properties and their PRE effects on proteorhodopsin

	Cu^{2+}-EDTA	Cu^{2+}-Tag	Gd^{3+}-TTAHA	Gd^{3+}-DOTA	Diamagnetic sample
Ligand denticity	6	6	10	8	–
Log K_s	18.9[a]	18.9[a]	19.0[b]	25.3[c]	–
Hydration number q	0	0	2[d]	1[e]	–
Optimal concentration	50 mM	15-fold	30 mM	2 mM	–
^1H T_1 [s] amide backbone	0.21 ± 0.1	0.14 ± 0.1	0.12 ± 0.1	0.08 ± 0.1	0.83 ± 0.1
^1H T_1 [s] pSB	0.24 ± 0.01	0.17 ± 0.03	0.14 ± 0.01	0.08 ± 0.03	0.86 ± 0.1
Opt. recycle delay [s]	1.05	0.7	0.6	0.4	4.2
Time saving	4.0	6.0	7.0	10.5	–
Relaxivity [$mM^{-1}s^{-1}$]	0.08 ± 0.02	0.07 ± 0.02[f]	0.22 ± 0.03	6.18 ± 0.23	–

[a] Stary 1963

[b] Wagner et al. 1997

[c] Kumar et al. 1994

[d] Ruloff et al. 1998

[e] Powell et al. 1996

[f] Just given for completeness. Since the labels are directly attached to GPR, a comparison with the other relaxivities is not meaningful

paramagnetism of metal binding proteins can be used to create paramagnetic relaxation enhancement (PRE), while the observation of pseudo-contact shifts (PCS) provides additional constraints in the solid-state (Bertini et al. 2010; Knight et al. 2012).

Although Cu^{2+}-EDTA has been successfully used, a choice of different paramagnetic dopants is highly desirable in order to meet the requirements imposed by diverse sample conditions (temperature, hydration, buffer system and pH), by protein-specific constraints (e.g. existing metal binding sites) or in case of membrane proteins by the lipid bilayer. Besides Cu^{2+}-EDTA (Ethylenediaminetetraacetic acid), also nitroxides or lanthanides could be applied. Amongst the latter, especially Gd^{3+} is of interest due to its seven unpaired electrons. It does not cause PCS since its magnetic susceptibility tensor is isotropic, but the size of the isotropic tensor component and its slow electronic relaxation rates cause large PRE. PRE effects by Gd^{3+} are larger than those reported for nitroxides and comparable to Cu^{2+} and Mn^{2+}(reviewed in (Otting 2010)). Gd^{3+}-complexes have been very popular as MRI contrast agents and many different chelators are available (Caravan et al. 1999). Here, TTAHA (N-Tris(2-aminoethyl)amine-N′,N′,N″,N″, N‴,N‴-hexitacetic acid) and DOTA (1,4,7,10-tetraaza-cyclodo-decane-tetraacetic acid) were chosen due to their high stability and ligand denticity (Table 1). In the following, PRE effects caused by Gd^{3+}-DOTA and Gd^{3+}-TTAHA will be compared with the established dopant Cu^{2+}-EDTA, which will be either added directly to the protein buffer or attached to cysteine side chains (Cu^{2+}-EDTA-tag) (Fig. 1). For this study, green proteorhodopsin (GPR), a pentameric/hexameric, heptahelical, 249 residue light-driven proton pump reconstituted into lipid bilayers, has been used in order to obtain realistic data on a large membrane protein [for a recent review see (Bamann et al. 2013)].

Methods

Expression, purification and reconstitution of green proteorhodopsin (GPR)

U-^{15}N-GPR and reversely labelled U-[^{13}C,^{15}N]$_{\backslash WHFLY}$-GPR were expressed in *E. coli* and purified as described before (Mehler et al. 2013). The protein was reconstituted in DMPC:DMPA (9:1) liposomes at a ratio of 2:1 (w/w). The pH was adjusted to 7.0 with 50 mM MES or to 9.0 with 50 mM Tris–HCl, unless stated otherwise. The amount of GPR placed in a 4 mm MAS rotor was between 5 and 10 mg.

Preparation of Cu^{2+}-EDTA

A stock solution of $(NH_4)_2$[Cu(EDTA)] was prepared by dissolving 1.0 eq. $CuSO_4$ (Aldrich) and H_4EDTA (Aldrich) (1.2 eq.) in H_2O. The pH was adjusted to 5–6 with NH_4OH. The complex was incubated at 4 °C over night before lyophilisation. Before usage the Cu^{2+}-EDTA complex was dissolved in NMR-buffer pH 9 (4 °C) and added to the sample in the tested concentrations. The sample was incubated at 4 °C for 10 min before ultracentrifugation and transferring into the MAS rotor.

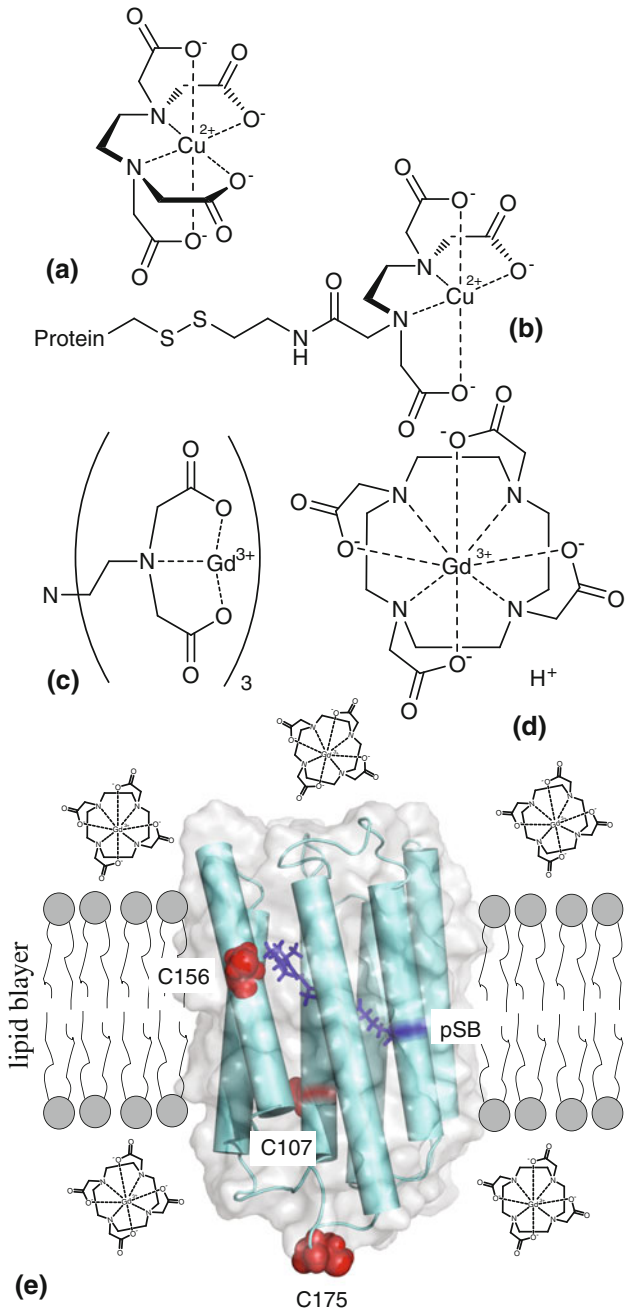

Fig. 1 Cu^{2+}-EDTA (**a**), Cu^{2+}-EDTA-tag bound via a disulfide bridge to cysteines in GPR (**b**), Gd^{3+}-TTAHA (**c**), Gd^{3+}-DOTA (**d**), structural model of GPR (Bamann et al. 2013) (**e**). The three accessible cysteines C107, C156 and C175 as well as protonated Schiff base (pSB) and retinal co-factor are highlighted

Cysteine side chain labelling of GPR by a Cu^{2+}-EDTA-tag

Site-specific labelling was done as described by Nadaud et al. (2007) with some modifications specific to GPR. GPR contains three cysteins (C107, 156, 175), which can be labelled (Hellmich et al. 2009). The protein was purified as described above but with the addition of 2 mM β-mercaptoethanol [β-ME] to all buffers. The Ni-NTA column was washed with 300 mM NaCl, 50 mM MES, 50 mM imidazole, 0.15 % DDM at pH 6. β-ME was removed in the last step by buffer exchange. The thiol-specific disulfide reagent, N-[S-(2-pyridylthio)cys-teaminyl]EDTA (EDTA-tag, Toronto Research Chemicals) pre-loaded with 1.1 mol eq. of Cu^{2+} was added in molar excess (1–30-fold) as aqueous solution. The sample was incubated overnight at 4 °C. Excess Cu^{2+}-EDTA-tag was removed by extensive washing with 300 mM NaCl, 50 mM MES, 50 mM imidazole, 0.15 % DDM at pH 6 on the Ni-NTA column before elution and reconstitution. Integrity of labelled samples was verified using optical spectroscopy (Fig. S3).

Preparation of Gd^{3+}-TTAHA

The Gd-complex was prepared according to published procedures (Ruloff et al. 1995). For the quality of the complex it was crucial to wash the Gd^{3+}-oxide-hydrate (Aldrich) extensively with 0.1 M NaOH and to let the complex build over night at 4 °C. After lyophilisation the Gd^{3+}-TTAHA complex was dissolved in NMR-buffer pH 9 (4 °C) and added to the sample in the tested concentrations. The sample was incubated at 4 °C for 10 min before ultracentrifugation and transferring into the MAS rotor.

Preparation of Gd^{3+}-DOTA

The Gd^{3+}-DOTA complex was bought from BOC Sciences (CAS no. 72573-82-1). The Gd^{3+}-DOTA powder was dissolved in NMR-buffer pH 9 (4 °C) and added to the sample in the tested concentrations. The sample was incubated at 4 °C for 10 min before ultracentrifugation and transferring into the MAS rotor.

NMR spectroscopy

All MAS NMR experiments were conducted using a Bruker 4 mm triple-resonance DVT HCN e-free probehead on a Bruker WB Avance I solid-state NMR spectrometer operating at a ^{1}H frequency of 600.13 MHz. 1D and 2D experiments were recorded using a sample spinning rate of 10 kHz with a 20 ms acquisition period unless stated otherwise. The total duty cycle was kept at 2–4 % of the experimental time. The temperature was set to 270 K at a maximum gas flow of 2000 l/h. Temperature equilibration was achieved by running a series of 'dummy' 1D CP-MAS experiments using the reduced recycle delay before real data acquisition. ^{1}H-T_1 values were determined by ^{15}N-detected saturation recovery experiments. ^{1}H transitions were saturated by a train of π/2 pulses followed by a variable saturation recovery delay before a ramped ^{1}H-^{15}N cross polarization step with a 1 ms contact time (Metz et al.

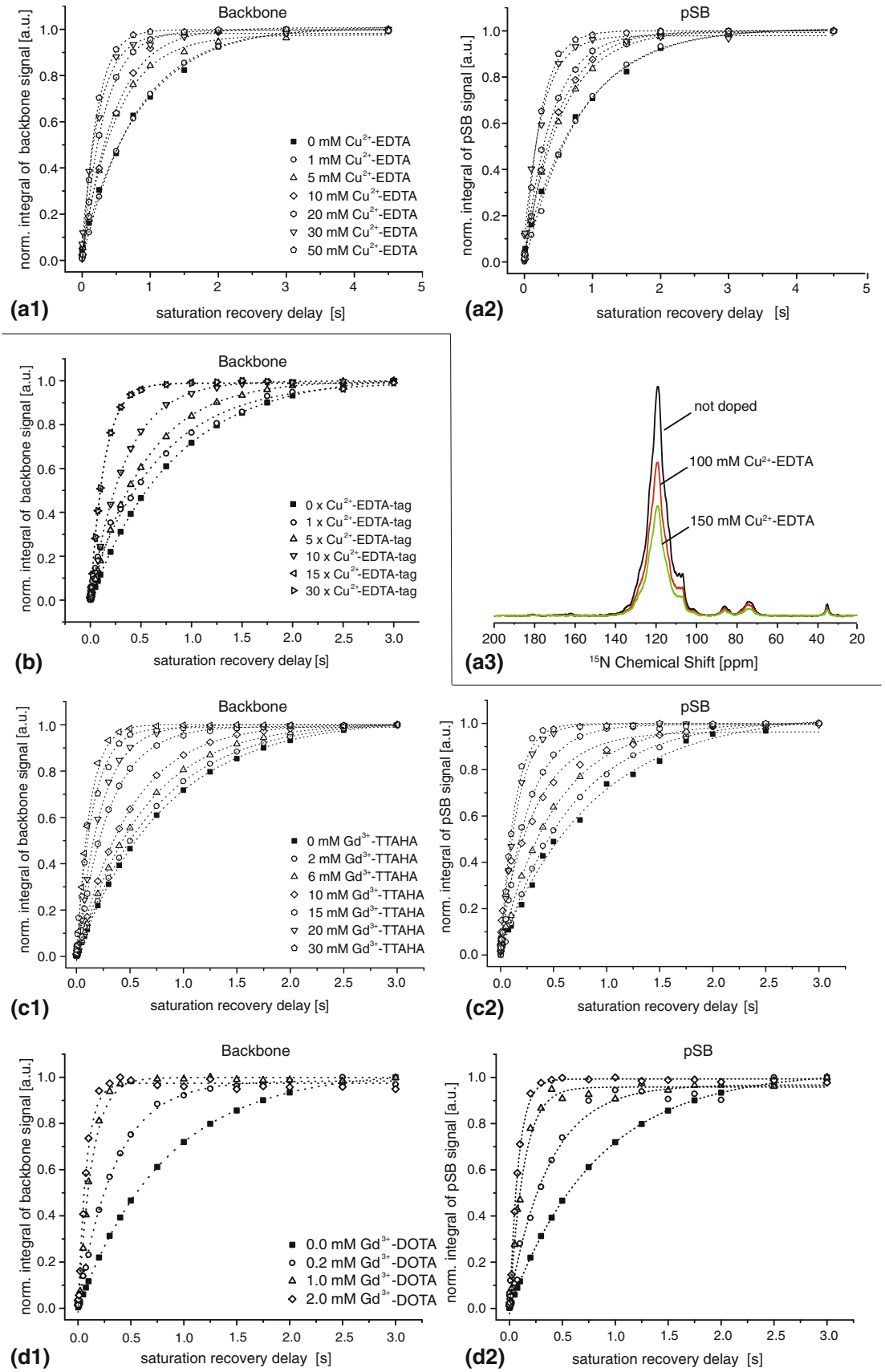
Backbone
norm. integral of backbone signal [a.u.]
saturation recovery delay [s]
0 mM Cu2+-EDTA
1 mM Cu2+-EDTA
5 mM Cu2+-EDTA
10 mM Cu2+-EDTA
20 mM Cu2+-EDTA
30 mM Cu2+-EDTA
50 mM Cu2+-EDTA
(a1)
pSB
norm. integral of pSB signal [a.u.]
saturation recovery delay [s]
(a2)
Backbone
norm. integral of backbone signal [a.u.]
saturation recovery delay [s]
0 x Cu2+-EDTA-tag
1 x Cu2+-EDTA-tag
5 x Cu2+-EDTA-tag
10 x Cu2+-EDTA-tag
15 x Cu2+-EDTA-tag
30 x Cu2+-EDTA-tag
(b)
not doped
100 mM Cu2+-EDTA
150 mM Cu2+-EDTA
15N Chemical Shift [ppm]
(a3)
Backbone
norm. integral of backbone signal [a.u.]
saturation recovery delay [s]
0 mM Gd3+-TTAHA
2 mM Gd3+-TTAHA
6 mM Gd3+-TTAHA
10 mM Gd3+-TTAHA
15 mM Gd3+-TTAHA
20 mM Gd3+-TTAHA
30 mM Gd3+-TTAHA
(c1)
pSB
norm. integral of pSB signal [a.u.]
saturation recovery delay [s]
(c2)
Backbone
norm. integral of backbone signal [a.u.]
saturation recovery delay [s]
0.0 mM Gd3+-DOTA
0.2 mM Gd3+-DOTA
1.0 mM Gd3+-DOTA
2.0 mM Gd3+-DOTA
(d1)
pSB
norm. integral of pSB signal [a.u.]
saturation recovery delay [s]
(d2)

◀ **Fig. 2** Saturation recovery curves for four different dopants and dopant concentrations. Normalized time traces are approximated with a mono-exponential function yielding ^{1}H-T$_1$. *Cu^{2+}-EDTA*: amide protons (**a1**), pSB (**a2**). The signal of the undoped sample (*black*) is significantly reduced after addition of 100 mM (*red*) and 150 mM (*green*) of Cu^{2+}-EDTA (**a3**). *Cu^{2+}-EDTA-tag*: Amide ^{1}H-T$_1$ times for five different samples incubated with 1-, 5-, 10-, 15- and 30-fold excess of the Cu^{2+}-EDTA-tag (**b**). *Gd^{3+}-TTAHA*: amide protons (**c1**), pSB (**c2**). *Gd^{3+}-DOTA*: amide protons (**d1**), pSB (**d2**). In all cases, the observed relaxation enhancement detected for the protons close to the pSB was similar to the average amide proton PRE (Table 1)

1994). High power proton decoupling (100 kHz) using TPPM (Bennett et al. 1995) was applied during ^{15}N acquisition (20 ms). The resulting saturation recovery curves (Fig. 2) can be described by a mono-exponential function to calculate ^{1}H-T$_1$. To obtain bulk amide ^{1}H-T$_1$, ^{15}N signals of the protein amide backbone were integrated from 124.5–104.5 ppm (Fig. 3c). The well-separated resonance of the protonated Schiff base at 182 ppm enabled to probe ^{1}H-T$_1$ of protons close to the Schiff base nitrogen in the hydrophobic core of GPR. ^{13}C-^{13}C through-space correlation spectroscopy was carried out using proton-driven spin diffusion (PDSD) (Szeverenyi et al. 1982). A series of 1D experiments was applied for temperature equilibration before recording the 2D spectra. All spectra were recorded with 1 ms CP contact time, 30 ms mixing time, 1358 complex data points and 15 ms acquisition and in the direct dimension and 825 data points and 10 ms acquisition in the indirect dimension. Typical 90° pulse lengths were 3 µs for ^{1}H, 4 µs for ^{13}C and 6 µs for ^{15}N. A recycle delay of 3–4 s, or shorter where mentioned, was used. Chemical shift referencing was carried out with respect to DSS through adamantane (40.49 and 31.47 ppm) and calculated for ^{15}N through the gyromagnetic ratio. Data processing was performed with Topspin 2.1. Data analysis was done with Sparky 3.113.

Results

Green proteorhodopsin ^{1}H-T$_1$ relaxation times as a function of dopant concentration were measured via saturation recovery experiments through ^{1}H-^{15}N cross polarization (Fig. 2). Bulk ^{1}H-T$_1$ was obtained by analysing changes in the integral signal intensity of the full ^{15}N amide backbone resonance, while more site-specific data were obtained via the protonated Schiff base signal (see spectrum in Fig. 3c). Under the experimental conditions applied here, a bulk ^{1}H-T$_1$ of 850 ms was found for the diamagnetic sample. ^{1}H-T$_1$ as a function of dopant concentration is plotted in Fig. 3a. A significant reduction is observed for all three dopants. It is worth noting hat Cu^{2+}-EDTA-tags attached to the three native cysteines C107, 156 and 175 in GPR, which are accessible for chemical labelling (Hellmich et al. 2009), also yield considerable PRE effects. A further increase of the concentration of the Cu^{2+}-EDTA-tag used for the labelling reaction did not further reduce the ^{1}H-T$_1$ times, showing that with 15-fold excess the labelling capacity of all three cysteines was reached (Table S2).

Our data reveal that very different concentrations are needed to achieve the comparable PRE effects, which becomes even more evident when comparing reciprocal plots (Fig. 3b): R$_1$ increases linearly with dopant concentration, but the relaxivity differs greatly. It is highest for Gd^{3+}-DOTA (6.18 $mM^{-1}s^{-1}$), followed by Gd^{3+}-TTAHA (0.22 $mM^{-1}s^{-1}$) and Cu^{2+}-EDTA (0.08 $mM^{-1}s^{-1}$). The linear dependence of R$_1$ shows that no paramagnetic quenching due to transversal PRE occurs within the plotted dopant concentration range, but signal loss for Cu^{2+}-EDTA has been observed above 100 mM (Fig. 2a3). Our data show that the maximal ^{1}H-T$_1$ reduction, which can be achieved for this typical membrane protein, is approximately tenfold for 2 mM Gd^{3+}-DOTA (80 ± 10 ms), sevenfold for 30 mM Gd^{3+}-TTAHA (120 ± 10 ms), sixfold for optimal cysteine labelling with Cu^{2+}-EDTA-tags and fourfold for 50 mM Cu^{2+}-EDTA (210 ± 10 ms). The pH dependence of all four dopants at their optimal concentrations was tested at pH 7 and 9, but no differences were observed (Table S1). The isolated signal of the protonated Schiff base (pSB) (Fig. 3c) also allowed doping effects within the hydrophobic core of GPR to be analysed (Fig. 2). These data follow the same trend as observed for the averaged amide ^{1}H-T$_1$ (Table 1) and show that the doping induced PRE extends uniformly into the centre of GPR.

Our data show that Gd^{3+}-DOTA is a highly efficient dopant. Therefore, the recycle delay time can be reduced significantly resulting in higher sensitivity as demonstrated for the optimal dopant concentration (Fig. 3c). For Gd^{3+}-DOTA, Gd^{3+}-TTAHA, Cu^{2+}-EDTA-tag and Cu^{2+}-EDTA, a 3.2-, 2.6-, 2.4-, and 2-fold improvement in SNR per unit time was obtained resulting in approximately 10-, 7-, 6- and 4-fold faster data acquisitions, respectively.

The effect of doping on chemical shifts and spectral resolution and its applicability to multidimensional solid-state NMR was analysed by comparing ^{13}C-^{13}C PDSD spectra of ^{13}C-labelled GPR with and without doping. The result for GPR doped with 2 mM Gd^{3+}-DOTA is shown in Fig. 4. The spectrum was recorded ten times faster, in less than 12 h instead of approximately 4 days on a non-doped sample. Neither significant peak shifts nor linebroadenings were detected. Similar results have been found for the other three dopants as shown in Figs. S1 and S2. Only in case of Cu^{2+}-EDTA-tags covalently attached to GPR, changes in some residues (e.g. D97, A116, A168) have been observed (Figs. 4c, S2).

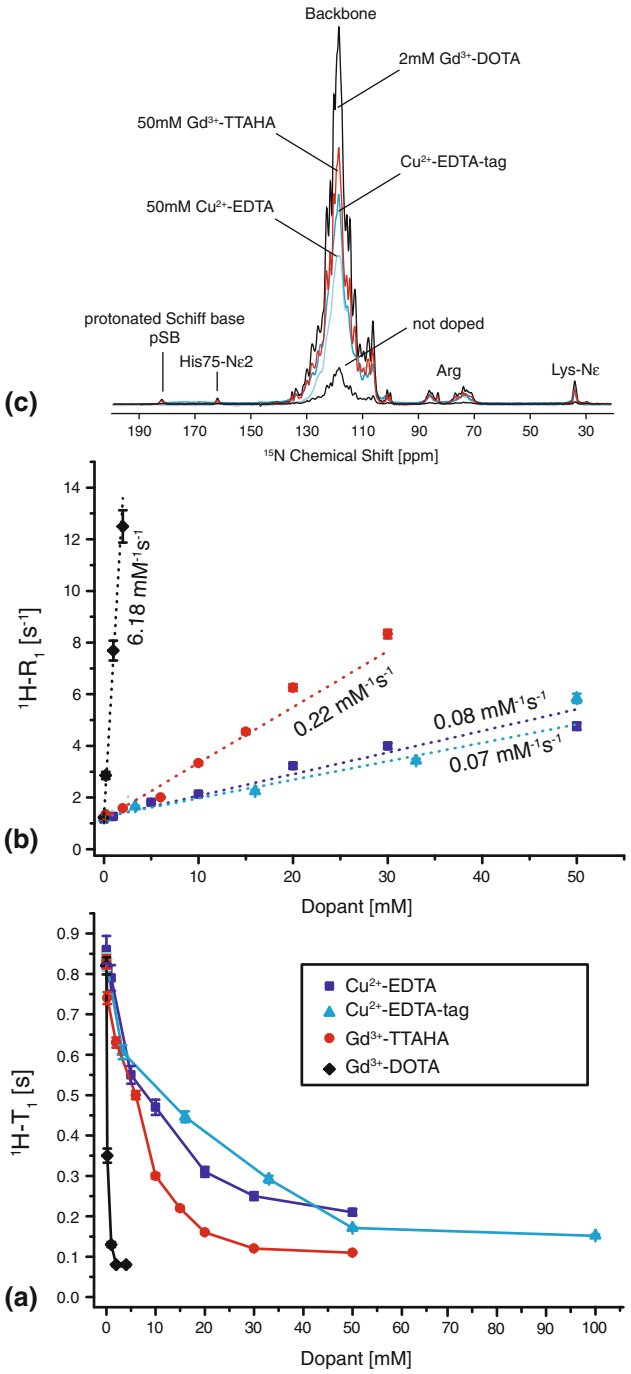

◀ **Fig. 3** Average amide ^{1}H-T_1 of GPR as a function of dopant concentration in linear (**a**) and reciprocal representation (**b**). The dopant relaxivities are obtained from the slope and are shown next to each curve. It is only given for completeness in case of Cu^{2+}-EDTA-tags, as the concentration just describes the values used for labelling (up to 30-fold excess, see Table S2). **c** Comparison of ^{15}N-CP MAS NMR spectra of doped and undoped GPR samples under identical experimental conditions. The recycle delay time was set to 5 × ^{1}H-T_1. When adding 50 mM Cu^{2+}-EDTA, 4 times more scans can be recorded in the same time resulting in fourfold better signal intensity and a twofold better SNR. Labelling GPR with Cu^{2+}-EDTA-tag (at saturated labelling capacity) results in 6 times more scans and a 2.4 better SNR. Doping with 30 mM Gd^{3+}-TTAHA provides 7-times more scans and a 2.6 better SNR. Doping with just 2 mM Gd^{3+}-DOTA accommodates 10 times more scans resulting in 3.2 better SNR

Discussion

NMR on paramagnetic systems in solution has been successfully established to yield additional structure constraints through PCS (Bertini et al. 2008) or PRE (Clore and Iwahara 2009). This concept has been extended into solid-state NMR, but it was also found that PRE could be used as well to accelerate data acquisition hence to improve SNR per unit time. For the purpose of condensed data acquisition in solid-state NMR on membrane proteins, the ideal doping agent should cause large ^{1}H-T_1 PREs but no PCSs nor line broadening, it should be stable, chemically inert and work at possibly low concentrations. Our data on GPR show that all four tested dopants fulfil these criteria to a certain extent. They yield a considerable PRE, which can be used to reduce the required NMR time while maintaining spectral resolution, once the optimal concentration has been found. Our data also show that the ^{1}H-T_1 PRE observed for the bulk amide protons is in all cases rather similar to the more site-specific values obtained for the protonated Schiff base in the core of the protein. This observation, together with the PDSD data (Figs. 4, S1), indicates uniform PRE within the protein, which is in line with current models for hydrated samples: the dopant relaxes protons on the protein surface, which will also affect other protons within the protein via spin diffusion mechanisms (Wickramasinghe et al. 2009). However, some important differences have been observed as well: In terms of SNR per unit time Gd^{3+}-DOTA and Gd^{3+}-TTAHA perform 1.6- and 1.3-times better than Cu^{2+}-EDTA (Figs. 2, 3). Especially for Gd^{3+}-DOTA, the differences are more pronounced when comparing relaxivity, which is 28 and 77 times higher compared to Gd^{3+}-TTAHA and Cu^{2+}-EDTA, respectively.

Cu^{2+}-EDTA was included in this study for comparison as it has been used extensively before on crystalline systems (Linser et al. 2007; Wickramasinghe et al. 2007), membrane proteins (Tang et al. 2011) and, by using Cu(II) with lipid chelators, on membrane-associated peptides (Yamamoto et al. 2010). Our data confirm its general usability, although relaxivity is lowest in our case. The fact that signal loss probably due to transversal PRE has been observed for higher Cu^{2+}-EDTA concentrations (Fig. 2a3) emphasizes the need to have a choice of dopants available in order to address different experimental requirements. Cu^{2+}-induced T_2-PRE effects have also been reported before (Nadaud et al. 2009; Su et al. 2012) and attaching paramagnetic complexes directly to the protein (or lipid) has been demonstrated to obtain long-range distance

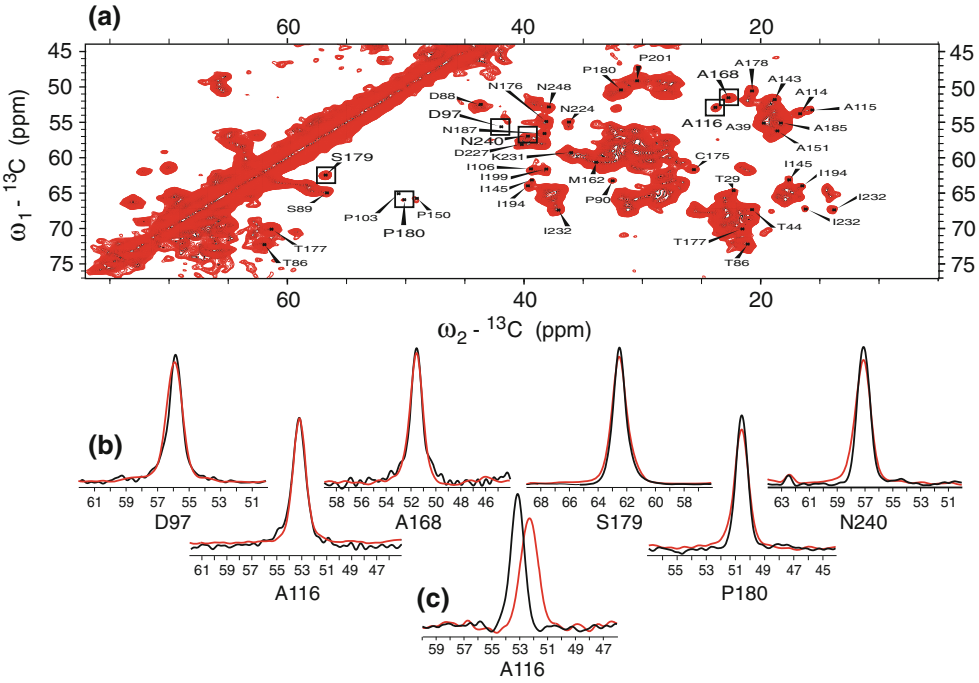

Fig. 4 Fast data acquisition by Gd^{3+}-DOTA doping. **a** Superposition of ^{13}C-^{13}C PDSD spectra of GPR non-doped (*black*) and doped with 2 mM Gd^{3+}-DOTA (*red*). The recycle delay was 4.2 s for the diamagnetic control sample and 0.4 s for the paramagnetic sample. The amount of sample and number of scans was the same for both spectra. **b** Cross sections along ω_2 for CA-CB crosspeaks show no doping induced linebroadening or chemical shift changes. Spectra for Cu^{2+}-EDTA, Cu^{2+}-EDTA-tag and Gd^{3+}-TTAHA are shown in Figs. S1 and S2. Only in case of covalently attached Cu^{2+}-EDTA, some chemical shift changes have been observed as shown here for A116 CA-CB crosspeak (**c**)

constraints (Nadaud et al. 2007, 2010). Here, the use of Cu^{2+}-EDTA-tags to shorten ^{1}H-T_1 is demonstrated. One limitation compared to the other three dopants is the required chemical modification of the target protein as well as the occurrence of local chemical shift changes probably due to steric or small PCS effects (Fig. 4, S2).

Both Gd^{3+} and Cu^{2+} have an isotropic or nearly isotropic magnetic susceptibility tensor and both show relatively long electron relaxation times (ns) (Benmelouka et al. 2007; Pintacuda et al. 2004). However, differences in potency can be expected as Cu^{2+} contains one but Gd^{3+} seven unpaired electrons, which made the latter the preferred ion for use in MRI contrast agents. Surprisingly, both of the Gd^{3+}-complexes used here show large differences in terms of relaxivity, which might be explained based on their chemical properties. In aqueous solution, paramagnetic relaxation of water contains contributions from directly coordinated water molecules ('inner sphere mechanism') and from those residing in a second coordination sphere ('second sphere mechanism') in exchange with bulk water. Furthermore, relaxation contributions from long-range dipolar interactions between the paramagnetic compound and nuclear spins depend on translational diffusion of ion and solvent and their closest distance ('outer sphere mechanism') (reviewed in (Caravan et al. 1999)). The contribution of the inner sphere mechanism to relaxivity is proportional to the number of directly bound water molecules (q), which is $q = 0$ for Cu^{2+}-EDTA, $q = 1$ for Gd^{3+}-DOTA and $q = 2$ for Gd^{3+}-TTAHA. In that respect, the latter should perform best, which has been indeed observed in aqueous solution (Ruloff et al. 1998). Obviously, a large number of parameters besides q are needed to describe all three mechanisms in order to explain or predict a trend in relaxivity. These include e.g. the rotational correlation time, water residence time, electronic relaxation time, translational diffusion and the distance from nuclei to the paramagnetic ion. It can be assumed that both Gd^{3+} complexes differ in rotational and translational diffusion due to their differences in charge and size but the other parameters are not known and the model only partially applies to the experimental situation described here (densely packed proteoliposomes, reduced amount of bulk water), since PRE might occur via protons in water molecules or directly via protons on the protein surface. Due to its size, Gd^{3+}-TTAHA might not get close enough to the protein's surface and so higher concentrations are necessary to reach a PRE comparable to Gd^{3+}-DOTA. The surprisingly high longitudinal relaxivity of Gd^{3+}-DOTA is therefore probably caused by a well-balanced optimum between hydration number, size, rotational and translation correlation times as well as electron relaxation properties.

Gd^{3+} not only causes longitudinal but also transversal PRE, but no significant linebroadening has been observed within the concentration range used here. According to the Salomon relaxation mechanism (Solomon 1955), both nuclear R_1 and R_2 due to dipolar couplings to unpaired electrons are proportional to $\left(\gamma_e^2\gamma_n^2/r^6\right)$. Since we analyse R_1-PRE of protons but detect ^{13}C or ^{15}N, R_2-PRE effects will be much less pronounced due to their lower gyromagnetic ratio. Furthermore, spin diffusion for ^{13}C or ^{15}N

is much slower than for protons, which also limits transfer from the surface into the interior of the protein.

Conclusions

Although lanthanide complexes were used before for generating PCS in solid-state and PRE in liquid-and solid-state NMR as structure constraints (Kervern et al. 2006; Yagi et al. 2010; Grobner et al. 1999), and Gd^{3+}-complexes were suggested as relaxation dopants in solid-state NMR (Mroue et al. 2012), this work is the first study actually demonstrating the suitability of Gd^{3+} for reducing measurement time in solid-state NMR spectroscopy. The very high relaxivity of Gd^{3+}-DOTA as shown here for proteorhodopsin, makes this dopant highly attractive for condensed data collection in membrane protein studies. Under the experimental conditions used here, SNR improvement per unit time by adding Gd^{3+}-DOTA is 1.6-times better than for Cu^{2+}-EDTA, while a 25-times lower concentration is needed. This lower dopant concentration helps reducing sample interference or heating effects. Furthermore, no linebroadening has been observed and PRE occurs within the whole protein. Shorten measurement time by paramagnetic doping is still the simplest and most universally applicable approach in solid-state NMR. Alternative methods based on band-selective excitation come at the expense of reduced data sets (Lopez et al. 2009) and dynamic nuclear polarization, the most powerful technique in terms of net signal enhancement, requires experiments at very low temperatures [for a review see Maly et al. (2008)]. One potentially damaging result of faster sampling is increased sample heating due to a higher probehead duty cycle. Possible solutions include paramagnetic doping in combination with fast MAS ($\geq$40 kHz) (Wickramasinghe et al. 2007, 2008, 2009) or sample deuteration (Linser et al. 2007) with low power decoupling. Here, sample heating was avoided by using a MAS probehead with reduced E-field (Stringer et al. 2005), which does allow using protonated samples, high power decoupling, moderate sample spinning rates and MAS rotors of conventional size. It has been shown for multidimensional experiments, that even faster data acquisitions are possible if non-uniform sampling is used together with paramagnetic doping (Sun et al. 2012). Doping membrane protein samples with Gd^{3+}-DOTA will not only be beneficial to gain a better SNR per time unit but faster data acquisition is also needed for time-resolved solid-state NMR, which will allow to obtain kinetic data of functional processes within membrane proteins.

Acknowledgments We are grateful to Dr. Jiafei Mao for comments to the manuscript, Dr. Andrea Lakatos for discussions and to Dr. Johanna Becker-Baldus for general NMR support. The work was funded by Bio-NMR and SFB 807.

References

Bamann C, Bamberg E, Wachtveitl J, Glaubitz C (2013) Proteorhodopsin. Biochim Biophys Acta. doi:10.1016/j.bbabio.2013.09.010

Benmelouka M, Borel A, Moriggi L, Helm L, Merbach AE (2007) Design of Gd(III)-based magnetic resonance imaging contrast agents: static and transient zero-field splitting contributions to the electronic relaxation and their impact on relaxivity. J Phys Chem B 111(4):832–840. doi:10.1021/jp0633289

Bennett A, Rienstra C, Auger M, Lakshmi K, Griffin R (1995) Heteronuclear decoupling in rotating solids. J Chem Phys 103:6951–6958

Bertini I, Luchinat C, Parigi G, Pierattelli R (2008) Perspectives in paramagnetic NMR of metalloproteins. Dalton Trans 29:3782–3790

Bertini I, Emsley L, Lelli M, Luchinat C, Mao J, Pintacuda G (2010) Ultrafast MAS solid-state NMR permits extensive 13C and 1H detection in paramagnetic metalloproteins. J Am Chem Soc 132:5558–5559

Caravan P, Ellison JJ, McMurry TJ, Lauffer RB (1999) Gadolinium(III) chelates as MRI contrast agents: structure, dynamics, and applications. Chem Rev 99(9):2293–2352

Clore GM, Iwahara J (2009) Theory, practice, and applications of paramagnetic relaxation enhancement for the characterization of transient low-population states of biological macromolecules and their complexes. Chem Rev 109(9):4108–4139. doi:10.1021/cr900033p

Ganapathy S, Naito A, McDowell C (1981) Paramagnetic doping as an aid in obtaining high-resolution carbon-13 NMR spectra of biomolecules in the solid state. J Am Chem Soc 103:6011–6015

Grobner G, Glaubitz C, Watts A (1999) Probing membrane surfaces and the location of membrane-embedded peptides by C-13 MAS NMR using lanthanide ions. J Magn Reson 141(2):335–339. doi:10.1006/jmre.1999.1894

Hellmich U, Pfleger N, Glaubitz C (2009) 19F-MAS NMR on proteorhodopsin: enhanced protocol for site-specific labeling for general application to membrane proteins. Photochem Photobiol 85:535–539

Kervern G, Pintacuda G, Zhang Y, Oldfield E, Roukoss C, Kuntz E, Herdtweck E, Basset JM, Cadars S, Lesage A, Coperet C, Emsley L (2006) Solid-state NMR of a paramagnetic DIAD-Fe-II catalyst: sensitivity, resolution enhancement, and structure-based assignments. J Am Chem Soc 128(41):13545–13552. doi:10.1021/ja063510n

Knight MJ, Pell AJ, Bertini I, Felli IC, Gonnelli L, Pierattelli R, Herrmann T, Emsley L, Pintacuda G (2012) Structure and backbone dynamics of a microcrystalline metalloprotein by solid-state NMR. Proc Natl Acad Sci USA 109(28):11095–11100. doi:10.1073/pnas.1204515109

Kumar K, Chang CA, Francesconi LC, Dischino DD, Malley MF, Gougoutas JZ, Tweedle MF (1994) Synthesis, stability, and structure of gadolinium (iii) and yttrium (iii) macrocyclic poly (amino carboxylates). Inorg Chem 33(16):3567–3575. doi:10.1021/ic00094a021

Linser R, Chevelkov V, Diehl A, Reif B (2007) Sensitivity enhancement using paramagnetic relaxation in MAS solid-state NMR of perdeuterated proteins. J Magn Reson 189(2):209–216. doi:10.1016/j.jmr.2007.09.007

Lopez JJ, Kaiser C, Asami S, Glaubitz C (2009) Higher sensitivity through selective (13)C excitation in solid-state NMR spectroscopy. J Am Chem Soc 131(44):15970–15971. doi:10.1021/ja904963n

Maly T, Debelouchina G, Bajaj V, Hu K, Joo C, Mak-Jurkauskas M, Sirigiri J, van der Wel P, Herzfeld J, Temkin R, Griffin R (2008) Dynamic nuclear polarization at high magnetic fields. J Chem Phys 128:052211–052219

Mehler M, Scholz F, Ullrich Sandra J, Mao J, Braun M, Brown Lynda J, Brown Richard CD, Fiedler Sarah A, Becker-Baldus J, Wachtveitl J, Glaubitz C (2013) The EF loop in green proteorhodopsin affects conformation and photocycle dynamics. Biophys J 105(2):385–397. doi:10.1016/j.bpj.2013.06.014

Metz G, Wu X, Smith S (1994) Ramped-amplitude cross polarization in magic-angle-spinning NMR. J Magn Reson A 110:219–227

Mroue KH, MacKinnon N, Xu J, Zhu P, McNerny E, Kohn DH, Morris MD, Ramamoorthy A (2012) High-resolution structural insights into bone: a solid-state NMR relaxation study utilizing paramagnetic doping. J Phys Chem B 116(38):11656–11661. doi:10.1021/jp307935g

Nadaud PS, Helmus JJ, Hofer N, Jaroniec CP (2007) Long-range structural restraints in spin-labeled proteins probed by solid-state nuclear magnetic resonance spectroscopy. J Am Chem Soc 129(24):7502–7503. doi:10.1021/ja072349t

Nadaud PS, Helmus JJ, Kall SL, Jaroniec CP (2009) Paramagnetic ions enable tuning of nuclear relaxation rates and provide long-range structural restraints in solid-state NMR of proteins. J Am Chem Soc 131(23):8108–8120. doi:10.1021/ja900224z

Nadaud PS, Helmus JJ, Sengupta I, Jaroniec CP (2010) Rapid acquisition of multidimensional solid-state NMR spectra of proteins facilitated by covalently bound paramagnetic tags. J Am Chem Soc 132(28):9561–9563. doi:10.1021/ja103545e

Otting G (2010) Protein NMR using paramagnetic ions. Annu Rev Biophys 39:387–405. doi:10.1146/annurev.biophys.093008.131321

Parthasarathy S, Nishiyama Y, Ishii Y (2013) Sensitivity and resolution enhanced solid-state NMR for paramagnetic systems and biomolecules under very fast magic angle spinning. Acc Chem Res. (epub ahead of print)

Pintacuda G, Moshref A, Leonchiks A, Sharipo A, Otting G (2004) Site-specific labelling with a metal chelator for protein-structure refinement. J Biomol NMR 29(3):351–361. doi:10.1023/B:JNMR.0000032610.17058.fe

Powell DH, NiDhubhghaill OM, Pubanz D, Helm L, Lebedev YS, Schlaepfer W, Merbach AE (1996) Structural and dynamic parameters obtained from O-17 NMR, EPR, and NMRD studies of monomeric and dimeric Gd3+ complexes of interest in magnetic resonance imaging: an integrated and theoretically self consistent approach. J Am Chem Soc 118(39):9333–9346. doi:10.1021/ja961743g

Renault M, Cukkemane A, Baldus M (2010) Solid-state NMR spectroscopy on complex biomolecules. Angew Chem Int Ed 49(45):8346–8357. doi:10.1002/anie.201002823

Ruloff R, Arnold K, Beyer L, Dietze F, Griinder W, Wagner M, Hoyer E (1995) Die Chelatbildung von N-Tris(2-aminoethy1)amin-N′, N′, N″, N″, N‴, N‴-hexaessigsaure (H, TTAHA) und N-(Pyrid-2-yl-methyl)-ethylen-diamin-N, N′, N′-triessigsaure (H, PEDTA) mit Gadolinium(III1)—Synthesen Komplexstabilitat und NMR-Relaxivitat. Z Anorg Allg Chem 621:807–811

Ruloff R, Muller RN, Pubanz D, Merbach AE (1998) A tripod gadolinium(III) poly(amino carboxylate) relevant to magnetic resonance imaging: structural and dynamical O-17 NMR and H-1 NMRD studies. Inorg Chim Acta 276(1–2):15–23

Solomon I (1955) Relaxation processes in a system of 2 spins. Phys Rev 99(2):559–565. doi:10.1103/PhysRev.99.559

Stary J (1963) Systematic study of solvent extraction of metal oxinates. Anal Chim Acta 28(2):132. doi:10.1016/s0003-2670(00)87211-6

Stringer JA, Bronnimann CE, Mullen CG, Zhou DH, Stellfox SA, Li Y, Williams EH, Rienstra CM (2005) Reduction of RF-induced sample heating with a scroll coil resonator structure for solid-state NMR probes. J Magn Reson 173(1):40–48. doi:10.1016/j.jmr.2004.11.015

Su Y, Hu F, Hong M (2012) Paramagnetic Cu (II) for probing membrane protein structure and function: inhibition mechanism of the influenza M2 proton channel. J Am Chem Soc 134(20):8693–8702. doi:10.1021/ja3026328

Sun SJ, Yan S, Guo CM, Li MY, Hoch JC, Williams JC, Polenova T (2012) A time-saving strategy for MAS NMR spectroscopy by combining nonuniform sampling and paramagnetic relaxation assisted condensed data collection. J Phys Chem B 116(46):13585–13596. doi:10.1021/jp3005794

Szeverenyi NM, Sullivan MJ, Maciel GE (1982) Observation of spin exchange by two-dimensional Fourier-transform C-13 cross polarization-magic-angle spinning. J Magn Reson 47(3):462–475

Tang M, Berthold D, Rienstra CM (2011) Solid-State NMR of a large membrane protein by paramagnetic relaxation enhancement. J Phys Chem Lett 2:1836–1841

Wagner M, Ruloff R, Hoyer E, Grunder W (1997) New gadolinium complexes as magnetic resonance imaging—Contrast agents. Zeitschrift Fur Naturforschung C-a J Biosci 52(7–8):508–515

Wickramasinghe NP, Kotecha M, Samoson A, Past J, Ishii Y (2007) Sensitivity enhancement in C-13 solid-state NMR of protein microcrystals by use of paramagnetic metal ions for optimizing H-1 T-1 relaxation. J Magn Reson 184(2):350–356. doi:10.1016/j.jmr.2006.10.012

Wickramasinghe NP, Shaibat MA, Jones CR, Casabianca LB, de Dios AC, Harwood JS, Ishii Y (2008) Progress in C-13 and H-1 solid-state nuclear magnetic resonance for paramagnetic systems under very fast magic angle spinning. J Chem Phys 128(5). doi:10.1063/1.2833574

Wickramasinghe NP, Parthasarathy S, Jones CR, Bhardwaj C, Long F, Kotecha M, Mehboob S, Fung LWM, Past J, Samoson A, Ishii Y (2009) Nanomole-scale protein solid-state NMR by breaking intrinsic H-1 T-1 boundaries. Nat Methods 6(3):215–218. doi:10.1038/nmeth.1300

Yagi H, Loscha KV, Su XC, Stanton-Cook M, Huber T, Otting G (2010) Tunable paramagnetic relaxation enhancements by [Gd(DPA)(3)](3-) for protein structure analysis. J Biomol NMR 47(2):143–153. doi:10.1007/s10858-010-9416-x

Yamamoto K, Xu J, Kawulka K, Vederas J, Ramamoorthy A (2010) Use of copper-chelated lipid speeds up NMR measurements from membrane proteins. J Am Chem Soc 132:6929–6931

Yamamoto K, Vivekanandan S, Ramamoorthy A (2011) Fast NMR data acquisition from bicelles containing a membrane-associated peptide at natural-abundance. J Phys Chem B 115(43):12448–12455. doi:10.1021/jp2076098